Inorganic Chemistry

Article

pubs.acs.org/IC

Controlling the Fluorescence Response of PET Sensors via the Metal-Ion π-Contacting Ability of the Fluorophore: Coumarin, a Weaker π Contacter

Joseph W. Nugent,[†] Joseph H. Reibenspies,[‡] and Robert D. Hancock*[,†]

[†]Department of Chemistry and Biochemistry, University of North Carolina—Wilmington,Wilmington, North Carolina 28403,United States

[‡]Department of Chemistry, Texas A&M University, College Station, Texas 77843, United States

Supporting Information

ABSTRACT: The π-contact hypothesis, that quenching of the fluorescence of complexes of photoinduced electron transfer sensors with heavy diamagnetic metal ions may be caused by π contacts between the metal ion and the fluorophore of the sensor, is examined with a study of the fluorescent properties of the sensor 4-[[bis(2-pyridinylmethyl)amino]methyl]-6,7-dimethoxy-1-benzopyran-2-one (cdpa) and the structures of its complexes with some metal ions. The coumarin-type fluorophore of cdpa is a weaker π-contact former than the anthracenyl fluorophore of the analogue adpa (*Inorg. Chem.* **2014**, *53*, 9014): only Ag^{I}, the strongest π contact former, quenches the fluorescence of cdpa, apart from paramagnetic Cu^{II} and Ni^{II}, which quench fluorescence by a redox mechanism not requiring π contacts. The structures of $[Ag(cdpa)NO_3]$ (**1**), $[Pb(cdpa)(NO_3)_2]$ (**2**), $[Zn(cdpa)(NO_3)_2]$ (**3**), $[Cd(cdpa)Cl_2]_2$ (**4**), $[Cd(cdpa)_2H_2O](NO_3)_2$ (**5**), and $[Hg(cdpa)_2H_2O](NO_3)_2$ (**6**) are reported. Structure **1** shows that Ag^{I} is the only metal ion studied that forms π contacts with the fluorophore of cdpa in the solid state: Ag···C η^2 π contacts of 3.083 and 3.095 Å, in line with quenching of the fluorescence of the Ag^{I}(cdpa) complex. In contrast, Pb^{II}, Zn^{II}, and Cd^{II} show chelation-enhanced fluorescence in their cdpa complexes, and the structures of **2**−**4** show that the fluorophore of cdpa in each case forms no π contacts. By contrast, the adpa complexes of Pb^{II} and Cd^{II} show π contacts with its more strongly π-contacting fluorophore (*Inorg. Chem.* **2014**, *53*, 9014). The structures of **5** and **6** show bis-complexes of cdpa: the coordination geometries of Cd^{II} and Hg^{II} are discussed in relation to the number of covalently bound donor atoms present. The preferred hapticity of π-contacted metal ions is evaluated from the literature structures, suggesting that d^{10} metal ions such as Ag^{I} and Hg^{II}, and tetragonally distorted Cu^{II} and Pd^{II}, prefer η^1 and η^2 π contacts, while more ionically bound metal ions such as K^{I}, Ba^{II}, and La^{III}, as well as $d^{10}s^2$ metal ions such as Tl^{I}, Pb^{II}, and Bi^{III}, prefer η^6 contacts.

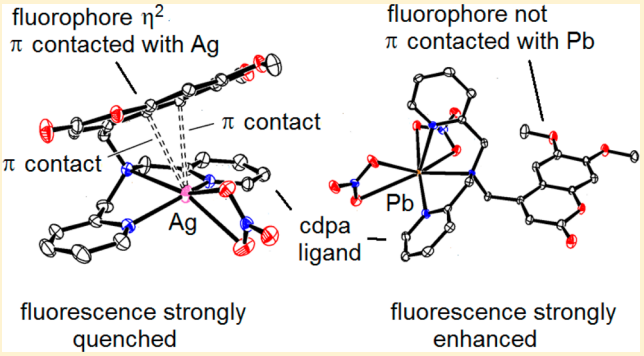

INTRODUCTION

In previous work, it was shown crystallographically[1−5] that there are π contacts between heavy diamagnetic metal ions such as Hg^{II}, Pb^{II}, Ag^{I}, and Pd^{II} complexed by adpa and the anthracenyl fluorophore of the sensor (see Figure 1 for abbreviations of ligands or sensors discussed in this paper). It was suggested, as supported by density functional theory (DFT) calculations, that π contacts with metal ions were mainly responsible for quenching of the fluorescence of such photoinduced electron transfer (PET) sensors in solution. Such quenching of the fluorescence is widely regarded as being due to large spin−orbit coupling constants (ζ), which stabilize the triplet state and so promote the nonradiative return of the excited electron to the ground state.[6] In contrast to the adpa complexes of the above heavy elements, the structure of the Zn^{II}(adpa) complex shows no π contacts:[3] there is a corresponding large increase in the fluorescence intensity of its adpa complex compared with the adpa free ligand, a chelation-enhanced fluorescence (CHEF) effect. Cd^{II} is borderline between the metal ions that π-contact strongly, such as Hg^{II}, Pb^{II}, Ag^{I}, and Pd^{II}, and Zn^{II}, which π-contacts only weakly, if at all, in solution. Cd^{II} thus shows a weaker CHEF effect than does Zn^{II}, which was suggested[2] to be due to the Cd^{II}(adpa) complex existing in solution as an equilibrium mixture of a π-contacted form (weakly fluorescent) and a non-π-contacted form (strongly fluorescent). The π-contact model of fluorescence quenching suggests[1−5] that a second ligand might bind to the Cd^{II}(adpa) complex and weaken or disrupt the π contact that is quenching the fluorescence. This leads to a new type of fluorescence sensor, where there is a large shift to shorter wavelength and an increase in the fluorescence intensity

Received: August 3, 2015
Published: October 1, 2015

DOI: 10.1021/acs.inorgchem.5b01766
Inorg. Chem. 2015, 54, 9976−9988

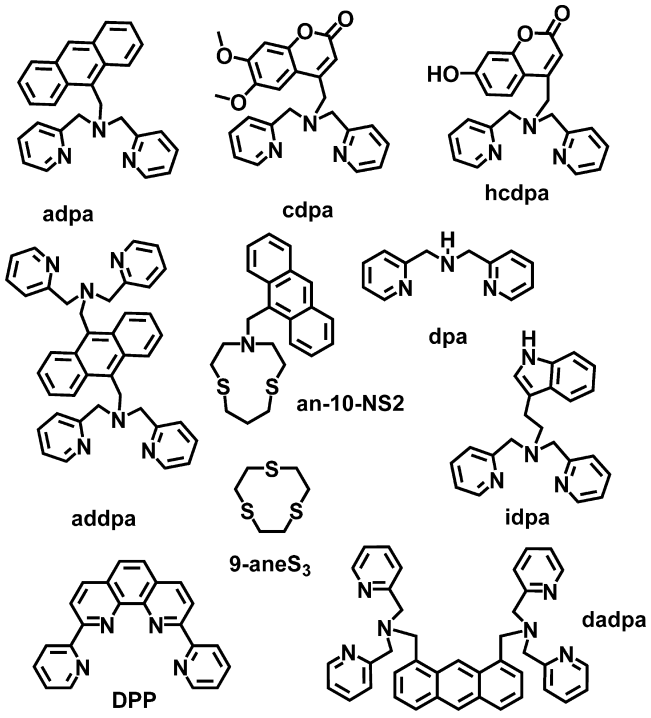

Figure 1. Ligands discussed in this paper.

when Cl^-, Br^-, SCN^-, or $S_2O_3^{2-}$ bind to the Cd^{II}(adpa) complex.[2,3] The π-contact model also predicts that with a more weakly π-contacting fluorophore, the Cd^{II} complex may not be strongly π-contacted in solution, and then there would be much less of a fluorescent response to added anions.

The idea that π contacts might be responsible for quenching of the fluorescence has also been explored by Ojida et al.,[7] who have reported the fluorescence properties of metal-ion complexes of dadpa (Figure 1). Crystal structures demonstrate the presence of a π-contact between Ag^I and the anthracenyl fluorophore of dadpa, so that Ag^I quenches the fluorescence of dadpa. Hitomi et al.[8] have shown that disruption of the Ag···C π contact with the anthracenyl fluorophore of the ligand an10-NS_2 by coordinating ethylene allows for the Ag^I(an10-NS_2) complex to act as a fluorescent sensor for ethylene and other alkenes.

In order to further investigate the π-contact model of quenching of the fluorescent PET sensors, it would be informative to investigate fluorophores that differ from anthracene in their metal π-contact forming ability. Gokel et al.[9] have used electrostatic potential maps, computed for fluorophores using wave-mechanical calculations, to indicate the metal π-contact forming ability; fluorophores with higher electron density in their π systems should be better π-contact formers. In Figure 2 are shown the electrostatic potential maps for naphthalene (which should be similar to anthracene) and coumarin, showing that coumarin has a lower electron density in its π system than does naphthalene and should therefore be a weaker π-contacter. The synthesis of a coumarin-based sensor, 4-[[bis(2-pyridinylmethyl)amino]methyl]-6,7-dimethoxy-1-benzopyran-2-one (cdpa) in Figure 1, and an extensive study of its fluorescence properties with some metal ions have already been reported by Lim and Bruckner.[10] The focus here will be on cdpa and the relationship between the occurrence of π contacts in cdpa complexes and of its fluorescence properties with metal ions. Judging from the frequency of occurrence of π-

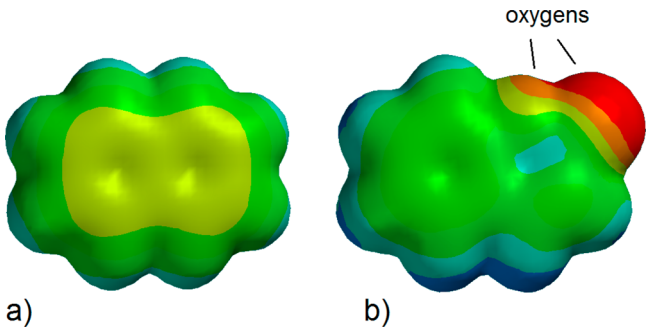

Figure 2. Electrostatic potential maps calculated using DFT (B3LYP 6-31G**) for (a) naphthalene and (b) coumarin. Red color = more negative electron density. Green to deep blue = more positive electron density. The more yellow color of the naphthalene π cloud suggests that naphthalene, and also anthracene, should be a stronger π-contact former with metal ions than coumarin. Maps plotted using the program *Spartan*.[21]

contacted structures in the CSD,[11] as well as DFT calculations, the order of the π-contacting ability of the metal ions considered here is $Ni^{II} \approx Zn^{II} \ll Cd^{II} < Pb^{II} < Hg^{II} < Pd^{II} \approx Cu^{II} \approx Ag^I$. This is not an ordering of the absolute strength of π-contact formation but includes the ease of displacement of a competing solvent molecule or other ligand by the aromatic group that forms the π contact.[3] In solution, the ability to form π contacts appears to be related to low solvation energies, so that such an ability is favored by metal ions of lower charge, particularly alkali-metal ions, Tl^I and Ag^I.[3] Because anthracene is a strong π-contact former, one finds that all of the above metal ions cluster together to form π contacts with adpa in solution, with only Zn^{II} and Ni^{II} not forming a π contact and the intermediate Cd^{II} displaying structures with and without π contacts. With a weaker π-contact former such as the dimethoxycoumarin fluorophore of cdpa, one expects the presence of π-contacted structures to be spread out, with a consequently greater ability to display a CHEF effect moving along the π-contacting strength series toward Ag^I, the most able π-contact former of those metal ions considered here. In other words, the weak π-contacter cdpa should make more apparent the above order of the π-contacting ability of metal ions, where the strong π-contacter adpa somewhat masks the order by π-contacting with all of the metal ions studied except for Zn^{II}.

An important aspect of quenching of the fluorescence of sensors such as adpa is distortion of the coordination geometry around heavy d^{10} metal ions such as Ag^I or Hg^{II}.[1] For these heavy d^{10} ions with a set of donor atoms that include both covalently and ionically bound donors, a quasi-linear structure is usually produced, with short M−N bonds to the two more covalently bound donors, in the case of adpa the sp^2-hybridized N donors of the two pyridyl groups, which are placed at roughly 180° to each other.[12−14] Long M−L bonds to the remaining donor atoms are found, which are placed at roughly right angles to the more covalently bound donors in the favored linear sites. Thus, long Hg−N bonds to the sp^3-hybridized central N donor of adpa are produced. This means that, even when the Hg···C π contact that is thought to quench the fluorescence of the complex is disrupted by coordination of a halide, the poor orbital overlap between the Hg atom and the N donor from the long Hg−N bond still allows a PET effect: little increase in the fluorescence intensity is observed. In contrast, Cd^{II} has a much weaker tendency toward such distortion of its coordination sphere: binding of Cl^-, Br^-, SCN^-, or $S_2O_3^{2-}$ to

DOI: 10.1021/acs.inorgchem.5b01766
Inorg. Chem. 2015, 54, 9976−9988

Table 1. Crystal Data and Details of the Structure Refinement for 1−6)

	1	2	3
empirical formula	$C_{24}H_{23}N_4O_7Ag$	$C_{24}H_{23}N_5O_{10}Pb$	$C_{24}H_{23}N_4O_{10}Zn$
fw	587.33	748.66	644.86
temperature (K)	110(2)	110(2)	110(2)
wavelength (Å)	0.71073	0.71073	0.71073
cryst syst	triclinic	monoclinic	triclinic
space group	$P\bar{1}$	$P2_1/c$	$P\bar{1}$
unit cell dimens			
a (Å)	9.0804(5)	10.9460(3)	7.897(3)
b(Å)	11.6555(6)	28.8405(7)	8.4500(4)
c (Å)	11.9969(7)	8.7430(2)	19.2843(8)
α (deg)	103.543(3)	90	81.422(2)
β (deg)	111.291(2)	109.2110(10)	87.890(2)
γ (deg)	93.928(2)	90	75.316(2)
volume (Å^3)	1133.51(11)	2606.36(11)	1231.02(9)
Z	2	4	2
final R indices [$I > 2\sigma(I)$]	R1 = 0.0256, wR2 = 0.0612	R1 = 0.0290, wR2 = 0.0636	R1 = 0.0577, wR2 = 0.1170
R indices (all data)	R1 = 0.0320, wR2 = 0.0650	R1 = 0.0341, wR2 = 0.0661	R1 = 0.1171, wR2 = 0.n
	4	**5**	**6**
empirical formula	$C_{24}H_{23}N_3O_6Cl_2Cd$	$C_{48}H_{48}N_8O_{15}Cd$	$C_{48}H_{48}N_8O_{15}Hg$
fw	680.79	1089.34	1177.53
temperature (K)	100(2)	110(2)	150(2)
wavelength (Å)	1.54178	0.71073	0.71073
cryst syst	triclinic	monoclinic	monoclinic
space group	$P\bar{1}$	$C2/c$	$C2/c$
unit cell dimens			
a (Å)	11.0395(4)	12.6124(11)	12.5438(11)
b(Å)	11.2652(4)	16.7766(14)	16.7705(14)
c (Å)	12.7588(4)	21.8695(19)	21.9486(19)
α (deg)	72.8307(18)	90	90
β (deg)	78.2274(17)	98.803(4)	98.684(4)
γ (deg)	79.4608(18)	90	90
volume (Å^3)	1471.29(9)	4572.9(7)	4564.3(7)
Z	2	4	4
final R indices [$I > 2\sigma(I)$]	R1 = 0.0288, wR2 = 0.0690	R1 = 0.0290, wR2 = 0.0679	R1 = 0.0253, wR2 = 0.0524
R indices (all data)	R1 = 0.0329, wR2 = 0.0650	R1 = 0.0375, wR2 = 0.0721	R1 = 0.0357, wR2 = 0.0560

Cd^{II} in its adpa complex weakens the Cd···C π contact that is quenching the fluorescence, the fluorescence intensity increases, and the Cd^{II}(adpa) complex can potentially act as a fluorescent sensor for the above anions.[2,3] In this paper, the coordination geometry of heavy d^{10} metal ions and how the problem of distortion of the coordination geometry to produce long Hg−N or Ag−N bonds that lead to a PET effect and quenching of the fluorescence might be overcome are further considered.

A study of the fluorescence of cdpa complexes is reported here, augmenting that reported for cdpa by Lim and Bruckner[10] in methanol (MeOH). Our studies were carried out in 50% MeOH/H_2O to make them comparable with our previous studies of adpa reported in the same solvent.[2−5] This is necessitated by the sensitivity of the fluorescence results to the solvent, particularly its hydrogen-bonding ability.[15,16] The π-contact forming abilities of the fluorophore of cdpa were investigated crystallographically in the complexes [Ag(cdpa)NO_3] (**1**), [Pb(cdpa)$(NO_3)_2$] (**2**), [Zn(cdpa)$(NO_3)_2$] (**3**), [Cd(cdpa)$Cl_2]_2$ (**4**), [Cd(cdpa)$_2H_2O](NO_3)_2$ (**5**), and [Hg(cdpa)$_2H_2O](NO_3)_2$ (**6**) in order to relate these to the fluorescence properties of the complexes.

EXPERIMENTAL SECTION

Materials. The ligand 4-[[bis(2-pyridinylmethyl)amino]methyl]-6,7-dimethoxy-1-benzopyran-2-one (cdpa) was synthesized following a literature method.[10] The metal salts $AgNO_3$ (Fisher), $CdCl_2{\cdot}2.5H_2O$ (Fisher), $Cd(NO_3)_2{\cdot}4H_2O$ (Riedel-de Haen), $Hg(NO_3)_2{\cdot}xH_2O$ (Alfa Aesar), $Pb(NO_3)_2$ (Fisher), and $Zn(NO_3)_2{\cdot}6H_2O$ (Aldrich) and metal perchlorates were obtained from VWR or Strem in ≥99% purity and used as received. All solutions were made up in deionized water (Milli-Q, Waters Corp.) of >18 MΩ·cm^{-1} resistivity, plus high-performance liquid chromatography grade methanol (MeOH) from Merck. Solutions were prepared in liquid chromatography/mass spectrometry grade MeOH and dimethyl sulfoxide (DMSO).

Elemental Analyses. The C and N elemental compositions were measured with a CE Elantech model NC 2100CHN analyzer.[17]

Synthesis of [Ag(cdpa)NO_3] (1). A total of 1 equiv of cdpa (33.3 mg, 0.08 mmol) was dissolved in 50:50 dichloromethane (DCM)/MeOH (6 mL) in a 30 mL sample vial. A solution of 1 equiv of $AgNO_3$ (13.6 mg, 0.09 mmol) in 20% DCM/MeOH (6 mL) was carefully added to the cdpa solution. The solutions were allowed to slowly diffuse into one another and then allowed to slowly evaporate through a perforated parafilm. After considerable evaporation, pale-yellow crystals deposited on the bottom of the glass. The solution was filtered off under vacuum, and the crystals were air-dried. **1**: pale-yellow crystals. Elem anal. Calcd for $C_{24}H_{23}AgN_4O_7$: C, 49.08; N, 9.54. Found: C, 49.19; N, 9.70.

DOI: 10.1021/acs.inorgchem.5b01766
Inorg. Chem. 2015, 54, 9976−9988

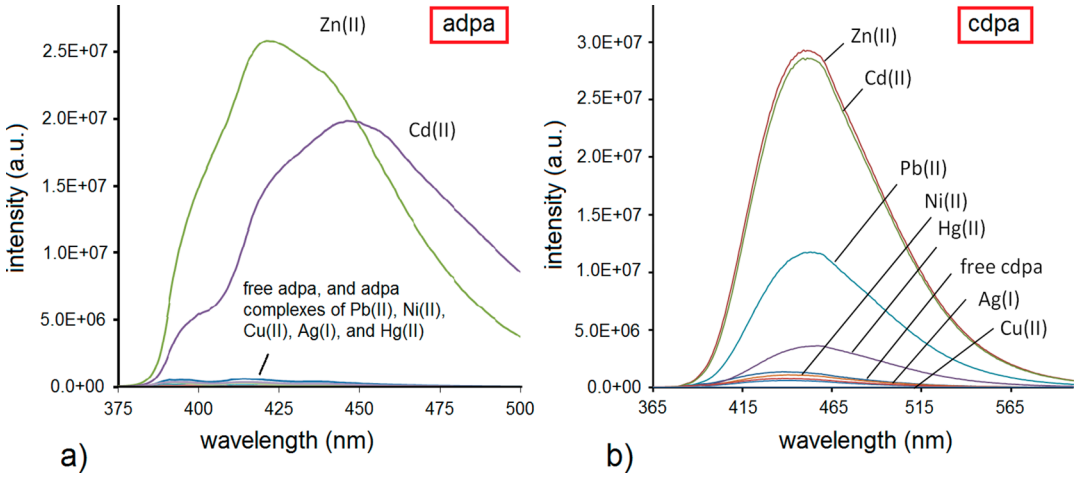

Figure 3. (a) Fluorescence spectra[3] of the complexes of a selection of metal ions with adpa (5×10^{-6} M) in 50% MeOH/H_2O. Note that nearly all of the metal ions quench the fluorescence of adpa, with only Zn^{II} showing a strong CHEF effect and Cd^{II} a somewhat weaker CHEF effect. (b) Fluorescence spectra of the complexes of a selection of metal ions with cdpa (5×10^{-6} M) in 50% MeOH/H_2O. Now Zn^{II} and Cd^{II} show nearly identical CHEF effects, with Pb^{II} and Hg^{II} showing weaker CHEF effects. Only Ag^{I} of the diamagnetic metal ions quenches the fluorescence of cdpa, and only Ag^{I} is shown here to form a π contact with cdpa. In each case, the spectrum of the complex is that obtained as a limiting spectrum when a sufficient concentration of the metal ion had been added to ensure complete formation of the complex.

*Synthesis of [Pb(cdpa)(NO$_3$)$_2$] (**2**).* A total of 1 equiv of cdpa (33.3 mg, 0.08 mmol) was dissolved in 10% DMSO/MeOH (7 mL) in a 30 mL sample vial, into which a solution of 1 equiv of $Pb(NO_3)_2$ (26.5 mg) dissolved in 2 mL of 10% DMSO/MeOH was added. The resulting solution in its vial was transferred to a larger jar, where it stood in about 5 mL of diethyl ether, and the lid of the jar was tightly closed. Diffusion of diethyl ether vapor into the solutions resulted in pale-yellow crystals. The solution was filtered off under vacuum, and the crystals were air-dried. Elem anal. Calcd for $C_{24}H_{23}PbN_5O_{10}$: C, 38.50; N, 9.35. Found: C, 38.38; N, 9.15.

*Synthesis of [Zn(cdpa)(NO$_3$)$_2$] (**3**).* A total of 1 equiv of cdpa (33.3 mg, 0.08 mmol) was dissolved in 20% DMSO/MeOH (5 mL) in a 30 mL sample vial, into which a solution of 1 equiv of $Zn(NO_3)_2 \cdot 6H_2O$ (23.8 mg) in MeOH (2 mL) was added. Use of the diethyl ether diffusion technique, as described for **2**, resulted in pale-yellow crystals, which were filtered off under vacuum and air-dried. Elem anal. Calcd for $C_{24}H_{23}ZnN_5O_{10}$: C, 47.50; N, 11.54. Found: C, 47.50; N, 11.09.

*Synthesis of [Cd(cdpa)Cl$_2$]$_2$ (**4**).* A total of 1 equiv of cdpa (33.3 mg, 0.08 mmol) was dissolved in 20% DMSO/MeOH (5 mL) in a 30 mL sample vial, into which a solution of 1 equiv of $CdCl_2 \cdot 2.5H_2O$ (18.2 mg) in MeOH (3 mL) was added. Use of the diethyl ether diffusion technique, as described for **2**, resulted in pale-yellow crystals, which were filtered off under vacuum and air-dried. Analysis of the bulk product proved problematic. Repeated syntheses (twice) and elemental analyses (four times) consistently gave results that fitted the product plus a H_2O molecule (calculated results are given in parentheses below). A mass spectrum did not give the molecular ion for the complex but only the free ligand plus other fragments. It is believed that the structure refers to a minority product crystal that had no H_2O molecule in the lattice. Elem anal. Calcd for $C_{24}H_{23}CdCl_2N_3O_4$ (H_2O): C, 47.98 (46.58); N, 6.99 (6.79). Found: C, 46.44; N, 6.33.

*Synthesis of [Cd(cdpa)$_2$H$_2$O](NO$_3$)$_2$ (**5**).* A total of 1 equiv of cdpa (33.3 mg, 0.08 mmol) was dissolved in 20% DMSO/MeOH (5 mL) in a 30 mL sample vial, into which a solution of 1 equiv of $Cd(NO_3)_2 \cdot 4H_2O$ (24.6 mg) in 20% DMSO/MeOH (4 mL) was added. Use of the diethyl ether diffusion technique, as described for **2**, resulted in pale-yellow crystals, which were filtered off under vacuum and air-dried. Elem anal. Calcd for $C_{48}H_{46}CdN_8O_{14}(H_2O)$: C, 52.92; N, 10.29. Found: C, 52.28; N, 10.17.

*Synthesis of [Hg(cdpa)$_2$H$_2$O](NO$_3$)$_2$ (**6**).* A total of 1 equiv of cdpa (33.3 mg, 0.08 mmol) was dissolved in 20% DMSO/MeOH (5 mL) in a 30 mL sample vial, into which a solution of 1 equiv of $Hg(NO_3)_2 \cdot xH_2O$ (27.4 mg) in 20% DMSO/MeOH (7 mL) was added. Use of the diethyl ether diffusion technique, as described for **2**, resulted in pale-yellow crystals, which were filtered off under vacuum and air-dried. Elem anal. Calcd for $C_{48}H_{46}HgN_8O_{14}$ (H_2O): C, 48.96; N, 9.52. Found: C, 48.62; N, 9.10.

Molecular Structure Determination. A Bruker D8-GADDS X-ray (three-circle) diffractometer was employed for crystal screening, unit cell determination, and data collection for structures **1**–**6**. The structures were solved by direct methods and refined to convergence.[18] Details of the structure determination are given in Table 1, and crystal coordinates and details of the structure determination of **1**–**6** have been deposited with the CSD (Cambridge Structural Database; see also the Supporting Information).[11] A selection of bond lengths and angles for **1**–**6** are given in Tables 2–7. The structures of **1**–**6** are shown in Figures 5–10.

Fluorescence Measurements. Excitation–emission matrix fluorescence properties were determined on a Jobin Yvon SPEX Fluoromax-3 scanning fluorimeter equipped with a 150 W xenon arc lamp and a R928P detector.[19] The instrument was configured to collect the signal in ratio mode with a dark offset using 5 nm band passes on both the excitation and emission monochromators. Replicate scans were generally within 5% agreement in terms of the intensity and within band-pass resolution in terms of the peak location. The fluorescence of the cdpa solutions was recorded in 50% MeOH/H_2O.

DFT Calculations. Modeling and DFT calculations were carried out using the program *Spartan*.[21] The B3LYP exchange-correlation functional was used for all DFT calculations,[22,23] the 6-31G* basis set[24] was used for the main-group elements, and the Lanl2DZ effective core potential was used for the metal ions.[25−27] The program *Hyperchem*, which allows for user-defined force constants, was used for molecular mechanics (MM) calculations.[28]

Formation Constants. Studies of the complex formation of cdpa with a variety of metal ions in 50% MeOH/H_2O were carried out by titrating 5×10^{-6} M solutions of cdpa at pH 6.4 (where the ligand is not protonated) with solutions of the metal ions to obtain limiting spectra corresponding to the fully formed mono ML complexes and to allow for the determination of log K values from variation of the fluorescence intensity as a function of the metal-ion concentration. pK_a (protonation constant) values in 50% MeOH/H_2O were determined by titrating 2×10^{-6} M solutions of cdpa with base between pH 2 and 10, following changes in the absorbance spectra as a function of the pH. The resulting variation in the absorbance or fluorescence intensity, depending on which type of spectroscopy was used to monitor the equilibria, was analyzed as a function of the metal-ion concentration or pH using *Excel*.[29] The program *HySS*[30] was used to model the

DOI: 10.1021/acs.inorgchem.5b01766
Inorg. Chem. 2015, 54, 9976−9988

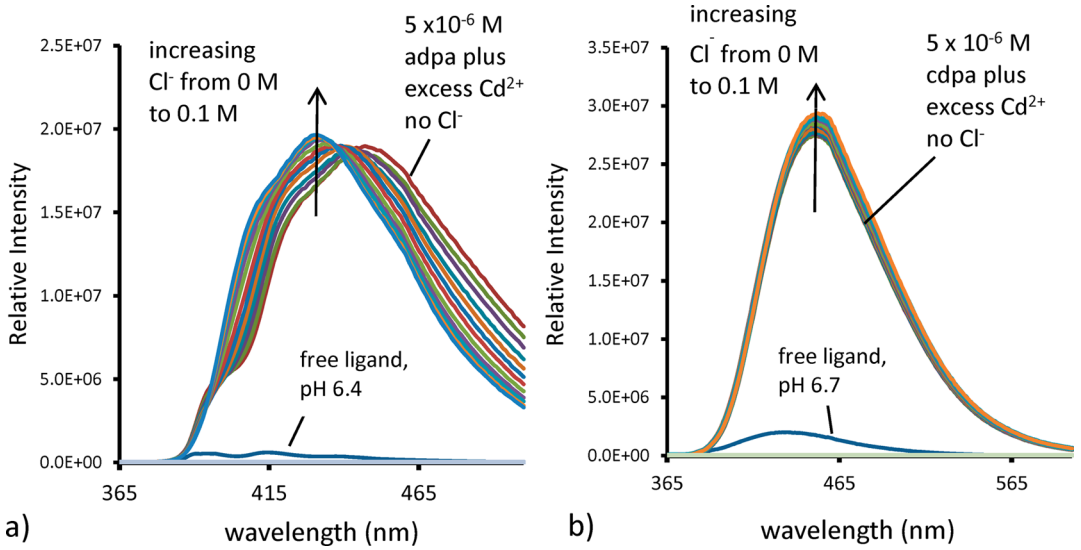

Figure 4. (a) Fluorescence spectra[3] of the Cd^{II}(adpa) complex (5×10^{-6} M) in 50% MeOH/H_2O titrated with NaCl. (b) Fluorescence spectra[3] of the Cd^{II}(cdpa) complex (5×10^{-6} M) in 50% MeOH/H_2O titrated with NaCl. Note that sufficient excess of Cd^{2+} was added to ensure complete formation of the complex in both cases.

equilibria and generate species distribution diagrams. UV−visible spectra were recorded using a Varian 300 Cary 1E UV−visible spectrophotometer controlled by Cary *Win UV Scan Application*, version 02.00(5), software. Fluorescence spectra were recorded as described above. A VWR sympHony SR60IC pH meter with a VWR sympHony gel epoxy semimicrocombination pH electrode was used for all pH readings, which were made in the external titration cell, with N_2 bubbled through the cell to exclude O_2 and CO_2. The pH meter was calibrated using standard acid−base titration methods, in which $E°$ for the cell was determined from a linear plot of E versus calculated pH.

RESULTS AND DISCUSSION

Fluorescence of cdpa Complexes. In Figure 3a are shown the fluorescence spectra of the adpa complexes with a selection of metal ions and in Figure 3b the fluorescence spectra of the cdpa complexes with the same metal ions, all in 50% MeOH/H_2O. It should be noted that these are the spectra of 5×10^{-6} M cdpa or adpa with a sufficient excess of metal ion in solution to ensure complete formation of the complex. The spectra reported for cdpa complexes by Lim and Bruckner[10] refer to 1:1 metal/cdpa mixtures and so may not reflect the spectra of the fully formed complexes. What one sees in Figure 3a is that, with the more strongly π-contacting anthracenyl fluorophore of adpa, the fluorescence is strongly quenched by all of the metal ions except Zn^{II} and Cd^{II}. The fluorescence of the Cd^{II}(adpa) complex is weaker than that of the Zn^{II}(adpa) complex, which was suggested[2,3] to occur because the Cd^{II}(adpa) complex exists in solution as a mixture of π-contacted (weakly fluorescent) and non-π-contacted (strongly fluorescent) forms. Turning the attention to Figure 3b, one sees that the Cd^{II}(cdpa) complex fluoresces virtually as strongly as does the Zn^{II}(cdpa) complex. This would be exactly as predicted by the π-contact model of fluorescence in PET sensors, if the weakly π-contacting coumarin fluorophore of the cdpa sensor does not form π contacts in solution with either the Zn^{II} or Cd^{II}(cdpa) complex.

One sees further in Figure 3b that the Pb^{II}(cdpa) complex now shows a moderately strong CHEF effect, whereas the Pb^{II}(adpa) complex does not. Similarly, Hg^{II} in its cdpa complex shows a modest CHEF effect, which is not observed[1] in the adpa complex. The powerfully π-contacting Ag^{I} ion completely quenches the fluorescence of both cdpa and adpa, as would be expected. One notes that the paramagnetic Cu^{II} and Ni^{II} ions almost completely quench the fluorescence of both adpa and cdpa, which is expected because the redox mechanisms involved do not appear to require the formation of a π contact.[6]

If the Cd^{II}(cdpa) complex is not present in significant proportion as a π-contacted form, then one predicts that, because there is little of the form containing fluorescence-quenching π contacts to be broken by coordinated anions such as Cl^-, the fluorescence intensity of the fully formed non-π-contacted Cd^{II}(cdpa) complex will not be much affected by added Cl^-. This is what is found, as shown in Figure 4a,b. In Figure 4a is shown the response of the fully formed Cd^{II}(adpa) complex to added Cl^- ion. One sees a large shift in the fluorescence peak maximum, which would allow for ratiometric sensing of Cl^-, and an increase in the fluorescence intensity. In contrast, in Figure 4b, for the Cd^{II}(cdpa) complex, the addition of Cl^- ion has little effect on the fluorescence of the complex. The small increase in the fluorescence intensity probably reflects driving of the equilibrium toward the complete formation of $[Cd(cdpa)Cl]^+$ at high Cl^- concentration according to eq 1, eliminating what small percentage of the Cd^{II}(cdpa) complex that might be π-contacted:

$$Cd^{2+} + cdpa + Cl^- \leftrightarrows [Cd(cdpa)Cl]^+ \quad (1)$$

The point of interest is whether the crystal structures of the cdpa complexes support the π-contact model of fluorescence in PET sensors.

Structure of 1. The structure of **1** is seen in Figure 5, and bond lengths and angles of interest for **1** are given in Table 2. The Ag is coordinated in the more usual[3] *mer* (meridional) fashion to the three N donors of the cdpa ligand. There are short Ag−N bonds to the two sp^2-hybridized N donors of the pyridyl groups of the ligand, averaging 2.26 Å, with a long Ag−N bond of 2.679 Å to the central sp^3-hybridized N donor of the ligand. The Ag−O bonds to a chelating nitrate are 2.412 and 2.705 Å. This type of structure is typical of the heavier d^{10} metal ions,[12−14] with two short bonds to the two sp^2-hybridized N

DOI: 10.1021/acs.inorgchem.5b01766
Inorg. Chem. 2015, 54, 9976−9988

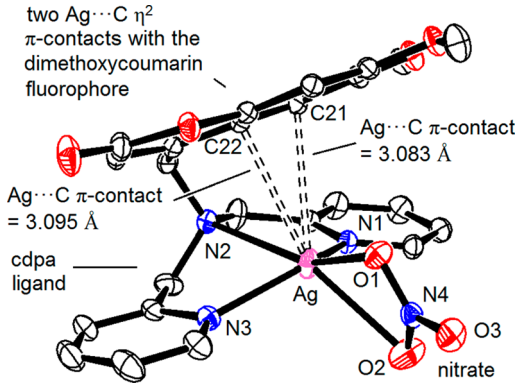

Figure 5. Structure of the Ag^{I}(cdpa) complex (**1**) showing the η^2 π contacts between Ag and C21 and C22 of the dimethoxycoumarin fluorophore. H atoms are excluded for clarity, and thermal ellipsoids are drawn at the 50% confidence level. Drawing made with *ORTEP*.[20]

donors, coordinated at roughly 180° to each other, with longer bonds to the remaining donor atoms. Of particular interest is the presence of two π contacts between the Ag^{I} ion and the dimethoxycoumarin fluorophore, of 3.083 and 3.095 Å. The structure of the Ag^{I}(cdpa) complex strongly resembles that of the Ag^{I}(adpa) complex, except that the latter has a η^1 contact with the anthracenyl fluorophore of adpa, with an Ag···C distance of 3.016 Å,[3] whereas the Ag^{I} ion in its cdpa complex has a η^2 π contact. The presence of π contacts between the coordinated Ag^{I} and the fluorophore of cdpa is consistent with the π-contact model of quenching of the fluorescence, in that coordination of Ag^{I} to cdpa leads to strong quenching of the fluorescence, as also occurs with the adpa complex, where an Ag···C π contact is present. One has to bear in mind, of course, that the long Ag−N bond to the sp^3-hybridized N donor of cdpa might also contribute to quenching of the fluorescence by a persistent PET effect.

Structure of **2**. The structure of **2** is seen in Figure 6, and bond lengths and angles of interest for **2** are given in Table 3. What is of particular importance in **2** is that the dimethoxycoumarin fluorophore does not form a π contact with the Pb^{II} ion in its cdpa complex, in agreement with the fact that Pb^{II} shows a CHEF effect with cdpa, as seen in Figure 3. In contrast, Pb^{II} forms a π contact[3] with the anthracenyl fluorophore of adpa and correspondingly strongly quenches the fluorescence of adpa. In **2**, there are Pb−N bonds to the two sp^2-hybridized N donors of the pyridyl groups of cdpa of 2.519 and 2.616 Å, with a Pb−N bond of 2.614 Å to the central sp^3-hybridized N donor of the ligand. The cdpa ligand is coordinated to the Pb^{II} ion in a less usual *fac* (facial) manner, which was also found for the adpa complex:[3] *fac* coordination allows all three N donors to coordinate near the favored coordination site opposite the inert pair of electrons of the Pb^{II} ion, the *antipodal* site.[3] The Pb ion forms four Pb−O bonds to two chelating nitrates with lengths ranging from 2.609 to 3.138

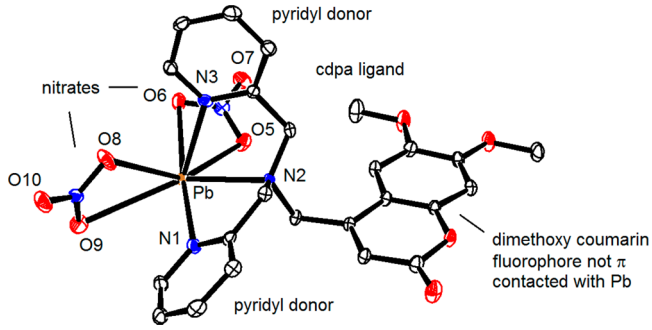

Figure 6. Structure of the Pb^{II}(cdpa) complex (**2**), showing the lack of a π contact between Pb^{II} and the dimethoxycoumarin fluorophore. H atoms are excluded for clarity, and thermal ellipsoids are drawn at the 50% confidence level. Drawing made with *ORTEP*.[20]

Table 3. Bond Lengths and Angles of Interest in the Structure of 2

Bond Length (Å)			
Pb1−O5	2.610(3)	Pb1−N1	2.616(3)
Pb1−N2	2.614(3)	Pb1−N3	2.520(3)
Bond Angle (deg)			
N1−Pb1−O8	76.89(10)	N2−Pb1−N1	64.01(10)
N3−Pb1−N1	100.57(11)	N3−Pb1−N2	64.62(11)

Å and also forms two PbO bonds to a bridging nitrate from an adjacent Pb with lengths of 2.816 and 2.836 Å. The position of a stereochemically active lone pair on the Pb^{II} ion is suggested[31−33] by a gap in the coordination geometry roughly opposite N2, the gap of which is surrounded by long Pb−O bonds ranging from 2.836 to 3.138 Å. The Pb−N bonds, which are closer to the antipodal site, are, as noted above, all much shorter, ranging from 2.519 to 2.616 Å.

Structure of **3**. The structure of **3** is seen in Figure 7a, and bond lengths and angles of interest for **3** are given in Table 4. The Zn is coordinated in a *mer* fashion to the three N donors of the cdpa ligand with Zn−N bonds to the two sp^2-hybridized N donors of the pyridyl groups of the ligand of 2.025 and 2.022 Å and with a Zn−N bond of 2.333 Å to the central sp^3-hybridized N donor of the ligand. The Zn forms three Zn−O bonds to one chelating and one nonchelating nitrate, with lengths ranging from 2.057 to 2.442 Å. The Zn···O6 contact, indicated as a dashed bond in Figure 7a, is rather long at 2.854 Å, which appears to be caused by steric interaction with the H atoms on the methylene linker holding the fluorophore in place. The dimethoxycoumarin fluorophore does not form a π contact with the Zn^{II} ion in its cdpa complex, in agreement with the fact that Zn^{II} shows a strong CHEF effect with cdpa in Figure 3. Zn^{II} is a weak π-contacter, so this is as expected: Zn^{II} also does not form a π contact with the anthracenyl fluorophore of adpa and so also shows a strong CHEF effect with adpa.[3]

Table 2. Bond Lengths and Angles of Interest in the Structure of 1

Bond Length (Å)					
Ag1−N1	2.2307(9)	Ag1−N2	2.6790(8)	Ag1−N3	2.2817(10)
Ag1−O1	2.4120(9)	Ag1−O2	2.7050(9)		
Bond Angle (deg)					
N1−Ag1−N3	133.43(3)	N1−Ag1−N2	71.16(4)		
N2−Ag1−N2	73.11(4)	N1−Ag1−O1	125.21(3)		

DOI: 10.1021/acs.inorgchem.5b01766
Inorg. Chem. 2015, 54, 9976−9988

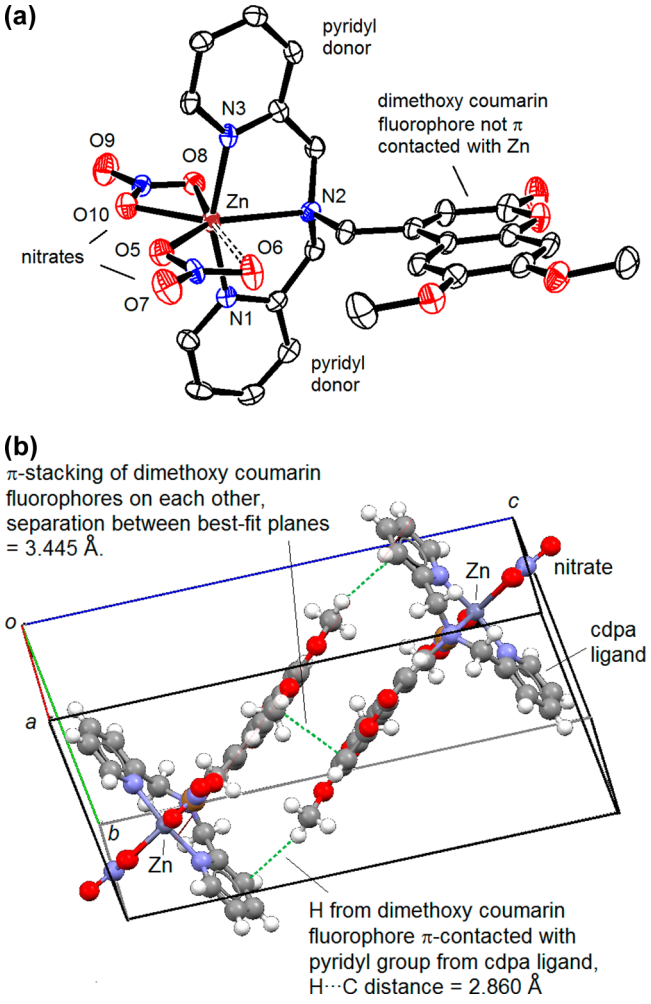

Figure 7. (a, top) Structure of the Zn^{II}(cdpa) complex (**3**), showing the lack of a π contact between Zn^{II} and the dimethoxycoumarin fluorophore. The nearer of the two nitrates is regarded as nonchelating because of the rather long Zn−O6 bond of 2.854 Å. H atoms are excluded for clarity, and thermal ellipsoids are drawn at the 50% confidence level. Drawing made with *ORTEP*.[20] (b, bottom) Unit cell of structure **3**, showing two $[Zn(cdpa)(NO_3)_2]$ individuals held together by π stacking of their dimethoxycoumarin fluorophores. Also shown is what appears to be a H···C π contact between an H atom from a methoxy group of the fluorophore and a pyridine from the other $[Zn(cdpa)(NO_3)_2]$ individual. Drawing made with *Mercury*.[11]

Table 4. Bond Lengths and Angles of Interest in the Structure of 3

Bond Length (Å)			
Zn1−O8	2.442(3)	Zn1−O10	2.113(3)
Zn1−N1	2.022(3)	Zn1−N2	2.333(3)
Zn1−O5	2.057(3)	Zn1−N3	2.024(4)
Bond Angle (deg)			
N1−Zn1−N2	78.33(13)	N1−Zn1−N3	155.74(13)
N3−Zn1−N2	78.23(13)	N3−Zn1−O5	99.68(13)

The crystal packing of **3** is of some interest, as seen in Figure 7b: the structure illustrates some other weak interactions that are important in structural chemistry, namely, π stacking of aromatic rings on each other[34−36] and H···C(aromatic) π contacts,[37] the structural features of which are observed in structures **1**−**6**. The unit cell of **3** is shown with two $[Zn(cdpa)(NO_3)_2]$ individuals held together by π stacking. The two dimethoxycoumarin fluorophores have best-fit planes separated by a C···C distance of 3.445 Å, which is typical for π stacking of aromatic groups.[36] The structure is held together by columns of dimethoxycoumarin fluorophores from one row of $[Zn(cdpa)(NO_3)_2]$ individuals π-stacked on columns of dimethoxycoumarin fluorophores from an opposing row of $[Zn(cdpa)(NO_3)_2]$ individuals. What may also be involved in controlling the structure of the crystal are H···C(aromatic) π contacts between H atoms on the methoxy groups of the fluorophores and C atoms from the pyridyl groups of the cdpa ligand. These H···C distances are (Figure 7b) 2.860 Å, somewhat less than the sum of the van der Waals radii of C and H. Such H···C(aromatic) π contacts appear to be important in biology,[37] where, for example, they may control molecular recognition of the carbohydrate groups responsible for determining A, B, and O blood group types.

Structure of 4. The structure of **4** is seen in Figure 8, and bond lengths and angles of interest for **4** are given in Table 5.

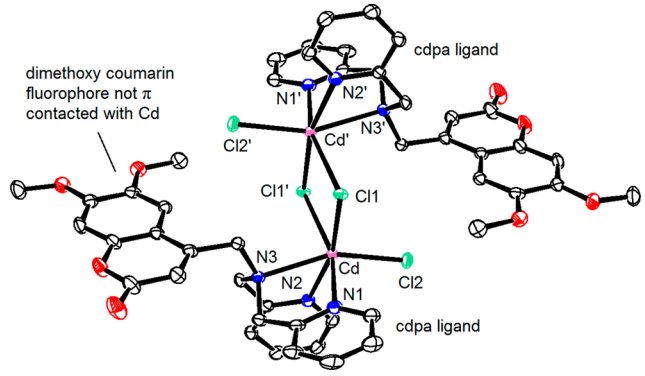

Figure 8. Structure of the **4** dimer, showing the non-π-contacted dimethoxycoumarin fluorophore. H atoms are excluded for clarity, and thermal ellipsoids are drawn at the 50% confidence level. Drawing made with *ORTEP*.[20]

Table 5. Bond Lengths and Angles of Interest in the Structure of 4

Bond Length (Å)			
Cd1−N1	2.365(2)	Cd1−N2	2.381(2)
Cd1−N3	2.487(2)	Cl1−Cd1′	2.6603(6)
Cd1−Cl1	2.6453(6)	Cd1−Cl2	2.4791(6)
Bond Angle (deg)			
N1−Cd1−N2	95.02(7)	N1−Cd1−N3	69.75(7)
N2−Cd1−N3	71.08(7)	N1−Cd1−Cl1	89.31(5)

The complex is a dimer with the two Cd^{II} ions held together by two bridging chloride ions. Each Cd^{II} is 6-coordinate, with three Cd−N bonds to cdpa ranging from 2.365 to 2.487 Å and three Cd−Cl bonds ranging from 2.479 to 2.660 Å. There are no π contacts between the Cd^{II} ions and the fluorophores of the cdpa ligands present, in accordance with the observation that Cd^{II} shows (Figure 3) a strong CHEF effect in solution with cdpa. One can argue, of course, that the chlorides coordinated to the Cd^{II} ions in **4** completely satisfy the most common coordination number of 6 found in the CSD for Cd^{II} complexes and so sterically preclude the formation of a π contact. Interestingly, **4** strongly resembles one of the complex species present in the corresponding structure of the adpa complex,[2]

DOI: 10.1021/acs.inorgchem.5b01766
Inorg. Chem. 2015, 54, 9976−9988

which is also a chloride-bridged dimer with no π contacts present. The latter Cd^{II}(adpa) complex unit cell also contains a monomeric species, [Cd(adpa)Cl_2], with a π-contacted anthracenyl fluorophore, which strongly supports the suggestion that the Cd^{II} can exist as both π-contacted and non-π-contacted species. It may be that the lack of any π-contacted form in the unit cell of **4** is indicative of the weaker π-contacting ability of the dimethoxycoumarin fluorophore of cdpa compared to the anthracenyl fluorophore of adpa because the adpa $CdCl_2$ structure contains forms with and without π contacts, while the cdpa $CdCl_2$ structure (**4**) contains only a non-π-contacted form.

Structure of ***5***. The structure of **5** is seen in Figure 9, and bond lengths and angles of interest for **5** are given in Table 6.

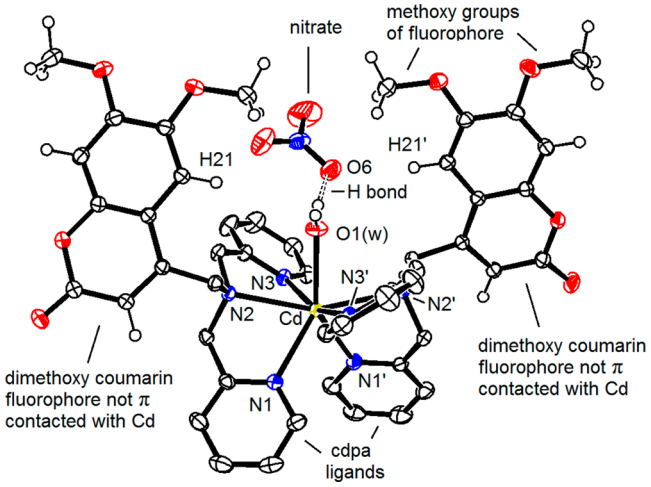

Figure 9. Structure of **5** showing the non-π-contacted dimethoxycoumarin fluorophores. H atoms are excluded for clarity, except for those on the dimethoxycoumarin fluorophores and on O1(w), the H_2O molecule coordinated to Cd. To avoid cluttering, only one of the two nitrate counterions is shown, that furthest from the observer, showing its hydrogen bond to an H atom on O1(w). Thermal ellipsoids are drawn at the 50% confidence level. Drawing made with *ORTEP*.[20]

Table 6. Bond Lengths and Angles of Interest in the Structure of 5

Bond Length (Å)			
Cd1–N1	2.3820(9)	Cd1–N2	2.5016(8)
Cd1–N3	2.3806(9)	Cd1–O1(w)	2.3294(12)
Bond Angle (deg)			
N1–Cd1–N3	110.29(3)	N2–Cd1–N3	70.49(3)
N1–Cd1–N2	69.79(3)	N2–Cd1–N2′	156.34(4)
N1–Cd1–O1(w)	139.52(2)	N2–Cd1–O1(w)	78.172(19)

The Cd^{II} ion in **5** is 7-coordinate, having two cdpa ligands coordinated to the Cd^{II} ion (average Cd–N = 2.421 Å), plus a H_2O molecule, with Cd–O = 2.329 Å. A coordination number of 7 is less common for Cd^{II}: a search of the CSD[11] yields 488 structures of Cd^{II} with six N donors coordinated to the Cd^{II} ion and a maximum coordination number of 6. On the other hand, there are only 10 structures[11] of Cd^{II} with six N donors and a seventh donor atom that is an O. One of these is the $Cd^{II}(dpa)_2$ complex,[38] where the unit cell contains one 6-coordinate $Cd^{II}(dpa)_2$ complex and a second 7-coordinate $Cd^{II}(dpa)_2$ individual that has a unidentate nitrate bound to the Cd. It thus appears that it is not energetically too unfavorable for the Cd^{II} ion to achieve an N_6O donor set with two dpa-type ligands such as cdpa bound to Cd^{II}. In order to gain some insight into why the Cd^{II} ion in **5** adopts a 7-coordinate structure, incorporating a H_2O molecule, MM calculations were carried out using the program *HyperChem*.[28] It was found that MM calculations reproduced the structure of **5** quite well, with the metal ion modeled with a "points on a sphere" approach, so that the metal ion was not constrained to any particular geometry. When the H_2O molecule was removed and the structure energy minimized, a cavity remained, formed by the two fluorophores arching over the site where the H_2O molecule could be coordinated. It thus appears that coordination of a H_2O molecule to the Cd^{II} ion in the cdpa bis-complex might be promoted by the architecture of the ligand, which provides a cage-type structure that creates a space in which the H_2O molecule can coordinate to the Cd^{II} ion, as shown in Figure 9.

The structure of **5** was somewhat unexpected because the crystals were grown with a 1:1 Cd/cdpa ratio. This has been found in our research to occur where bulky ligands such as DPP, rather hydrophobic on what will be the outside of the complex, are used for crystal growing in a more polar solvent such as MeOH. The 1:1 M/L mixtures produce crystals containing what must be the less soluble bis-complexes of 2,9-di(pyrid-2-yl)-1,10-phenanthroline (DPP) with both Zn^{II} and Cd^{II}.[39,40]

Solutions that are 1:1 in metal ions and ligands such as adpa and cdpa are used in crystal-growing experiments, or in fluorescence studies, with the belief that one has only the ML complex present in solution. The structure of **5** raises the question of what species are actually present in a 1:1 solution of adpa or cdpa with a metal ion. An indication of this can be gained from the log K_1 and log K_2 values available[33,42] for a range of metal ions with the dpa ligand in aqueous solution, as seen in Table 8. The log K_1 and log K_2 values reported by Anderegg et al.[42] for dpa complexes were used in the species distribution modeling program *HySS*[30] to calculate the percent of total Cd^{II} in a 1:1 solution of Cd^{II} and dpa (2×10^{-5} M) that would be present as ML and ML_2 complexes. One sees in Table 8 that this is strongly dependent on log (K_1/K_2). If log (K_1/K_2) is close to 3 or above, the percentage of M present as ML_2 is very small. Thus, for metal ions such as Zn^{II}, Pb^{II}, and Ag^{I}, log (K_1/K_2) for dpa is close to 3, and so the concentration of ML_2 species in a 1:1 M/dpa solution will be very low, which should also be the case for the cdpa complexes, so that crystallization produces the ML species. For Cd^{II}, log (K_1/K_2) for the dpa complex is low at only 1.03, and there should be some 13.9% of the total Cd^{II} present as the ML_2 complex in a 1:1 Cd^{II}(dpa) solution. A similar result for Cd^{II} with cdpa would account for crystallization of the cdpa bis-complex from a 1:1 Cd^{II}(cdpa) solution.

Structure of ***6***. The structure of **6** is shown as a space-filling drawing in Figure 10, and bond lengths and angles of interest for **6** are given in Table 7. **6** is isomorphous with **5**. A comparison of the bond lengths and angles in Tables 6 and 7 shows how similar the two complexes are: the Cd–N bond lengths, for example, average 2.411 Å, while the Hg–N bond lengths average 2.441 Å. The slightly longer Hg–N bonds are in accordance with the greater ionic radius for Hg^{II} of 1.02 Å for 6-coordination compared to 0.96 Å for Cd^{II}.[43] The structure of **6** here illustrates an important fact about the structure of Hg^{II} complexes. When the set of donor atoms bound to Hg^{II}

DOI: 10.1021/acs.inorgchem.5b01766
Inorg. Chem. 2015, 54, 9976–9988

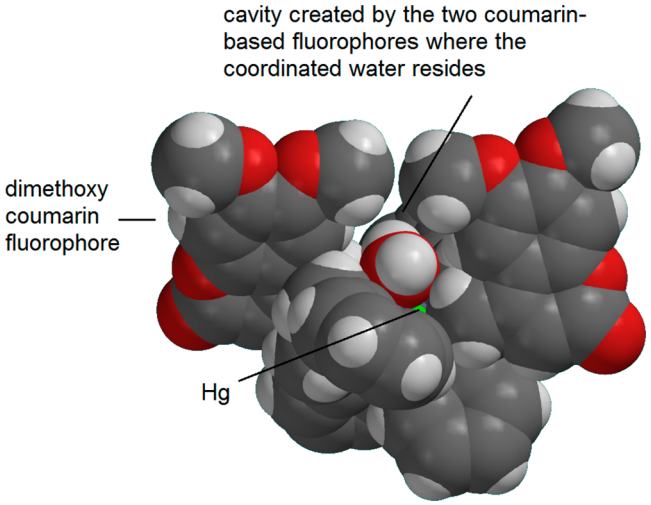

Figure 10. Space-filling drawing of **6**, showing the non-π-contacted dimethoxycoumarin fluorophores. The drawing shows how the two fluorophores are oriented so as to create a cavity above the Hg atom, which is occupied by the H_2O coordinated to the Hg. This structure is isomorphous with the Cd^{II} analogue, structure **5**. Drawing made with *Spartan*.[21]

Table 7. Bond Lengths and Angles of Interest in the Structure of 6

Bond Length (Å)			
Hg1–N1	2.4090(14)	Hg1–N2	2.5331(13)
Hg1–N3	2.3827(14)	Hg1–O1(w)	2.484(2)
Bond Angle (deg)			
N1–Hg1–N3	111.44(5)	N2–Hg1–N3	70.34(4)
N1–Hg1–N2	69.62(4)	N2–Hg1–N2′	153.99(6)
N1–Hg1–O1(w)	138.31(2)	N2–Hg1–O1(w)	76.99(3)

contains some donor atoms producing M–L bonds of high covalence and others that are more ionic, there is usually distortion to produce a quasi-linear structure as discussed above.[12−14] When all six donor atoms form Hg–L bonds of equally high covalence, then a more regular structure is formed with all Hg–L bonds of very similar length and also similar to the Cd^{II} analogue. Thus, for example, the six M–N bonds in the dpa bis-complexes of Hg^{II} are of similar length and average 2.416 ± 0.075 Å[44] compared to 2.360 ± 0.016 Å in the Cd^{II} analogue:[45] in the $Hg^{II}(9\text{-ane-}S_3)_2$ complex, the six Hg–S bonds are similar in length and average 2.682 Å, ± 0.023 Å[46] while in the Cd^{II} analogue, the Cd–S bonds average 2.658 ± 0.004 Å.[47] It is only with six covalently bound donor atoms bound to both Hg^{II} and Cd^{II} that the usual structural similarity between complexes of pairs of the heavier metal ions in the same group in the d-block elements, such as Pd^{II} and Pt^{II}, or Rh^{III} and Ir^{III}, becomes apparent with Cd^{II} and Hg^{II}.

The fluorophores in structures **5** and **6** form no π contacts with either Cd^{II} or Hg^{II} in their cdpa bis-complexes: the π-contact hypothesis concerning quenching of the fluorescence of PET sensors thus predicts that both of these complexes should fluoresce strongly in solution. In the case of the Cd^{II}(cdpa) mono-complex, the weakly π-contacting Cd^{II} should not form a strong π contact with the weakly π-contacting fluorophore. In contrast, Hg^{II} is a strong π-contacter, being between Pb^{II} and Ag^{I} in the π-contacting strength series discussed above. Pb^{II} shows a moderately strong CHEF effect with cdpa, as seen in Figure 3b, which is ascribed to the Pb^{II}(cdpa) complex existing in solution as an equilibrium mixture of π-contacted (weakly fluorescent) and non-π-contacted (strongly fluorescent) species. One would thus expect Hg^{II} to be better at forming π contacts than Pb^{II}, and so in the mono-complex, it shows weaker fluorescence than Pb^{II}, as seen in Figure 3b.

Formation Constants of cdpa Complexes. The formation constants determined here in 50% MeOH/H_2O for cdpa complexes with a selection of metal ions are seen in Table 9. The protonation constants reported were determined preferentially by absorbance spectroscopy: it was found that variation of the fluorescence spectral intensities with the pH

Table 9. Values of the log K_1 and pK_a Values, for adpa and cdpa, Determined in 50% MeOH/H_2O at 25 °C[a] and the log K_1 Values for dpa Reported in an Aqueous Solution

	Lewis acid					
	Cd^{II}	Zn^{II}	Ag^{I}	Pb^{II}	Hg^{II}	H^+
log K_1(dpa)[b]	6.40	7.63	5.46	6.00		7.20
log K_1(adpa)	4.44	6.01	6.38	4.06	~16[c]	6.01
log K_1(cdpa)	3.62	4.4	5.27	2.47	11.1	4.59

[a]The log K_1 values were determined by fluorescence spectroscopy, while the pK_a values were determined by absorbance spectroscopy. [b]In aqueous solution, ref 42. [c]From ref 1.

Table 8. Values of log K_1 and log K_2 for Dipicolylamine (dpa) Complexes, in Aqueous Solution,[41,42] Showing the Percentage of Mono (ML) and Bis (ML_2) Complexes Present for Each Metal Ion in a 1:1 Solution of the Metal Ion and dpa, Each 2 × 10^{-5} M, at pH 7.0, As Calculated Using the Program *HySS*[30]

	metal ion						
	Ni^{II}	Cu^{II}	Ag^{I}	Zn^{II}	Cd^{II}	Hg^{II} [a]	Pb^{II}
log K_1(dpa)	9.30	13.85	5.46	7.63	6.40	(11.1)	6.00
log K_2(dpa)	7.30	4.6	2.7	4.52	5.36	(8.5)	2.55
log (K_1/K_2)	2.00	9.3	2.8	3.11	1.04	(2.6)	3.45
% of M uncomplexed	0.4	0.001	46.0	5.6	25.2	(65.1)[b]	28.4
% of M as ML	83.2	99.9	52.3	92.3	60.9	(0.2)	69.9
% of M as ML_2	16.4	0.1	1.7	2.1	13.9	(34.7)	1.7

[a]These are results obtained here for Hg^{II} with cdpa in 50% MeOH/H_2O. For the Hg^{II}(dpa) complex, log K_1 has not been reported, with only log β_2 given as 22.2.[41,42] [b]The very high percentage of Hg^{II} left uncomplexed by cdpa is present as $Hg(OH)_2$ in solution, which results from the equilibrium $2Hg(cdpa)^{2+} + 2OH^- \leftrightarrows Hg(cdpa)_2^{2+} + Hg(OH)_2$ at pH 7.0. The latter equilibrium accounts for the very small percentage of Hg^{II} present as the mono-complex $Hg(cdpa)^{2+}$. A value of log β_2 = 21.6 for formation of the $Hg(OH)_2$ species in a 50% MeOH/H_2O solution was used in the calculations on the Hg^{II}(cdpa) system, the determination of which will be reported elsewhere.

DOI: 10.1021/acs.inorgchem.5b01766
Inorg. Chem. 2015, 54, 9976−9988

that might be used for pK_a analysis was somewhat erratic, as can occur with hydrogen-bonding structures that affect the intensity in a solvent such as 50% MeOH/H_2O.[15,16] The formation constants for the metal cdpa complexes were determined as reported previously[1,3] for adpa by titration of a 5×10^{-6} M cdpa solution with a metal-ion solution, with monitoring of the equilibrium by measurement of the fluorescence spectra: the intensity of these spectra were much better behaved than those related to the pK_a determination. Also shown in Table 9 for comparison are the formation constants for dpa (in aqueous solution)[42] and adpa (in 50% MeOH/H_2O) complexes.[1,3] The fact that the log K_1 values for the dpa complexes are reported in an aqueous solution should not make a great difference because it has been found that log K_1 values for 50% MeOH/H_2O and H_2O are quite similar.[5] One sees that the order of stability for most metal ions with the three ligands is dpa > adpa > cdpa. This might relate to some extent to the greater basicity of the central N donor of each ligand because the pK_a values vary in the same order. An exception is Ag^I, where it is found that the adpa complex is considerably more stable than the dpa complex, which is slightly more stable than the cdpa complex. One would suggest that this reflects the strength of the π contact formed by Ag^I with the anthracenyl fluorophore, which overrides the lower basicity of the central N of adpa. Although log K_1 for the cdpa complex of Ag^I is slightly less than log K_1 for the dpa complex, this is in contrast to the large drop in log K_1 from the dpa to cdpa complex for all of the other metal ions, suggesting again a degree of stabilization of the Ag^I(cdpa) complex by the formation of a π contact with the fluorophore of cdpa. No log K_1 value for Hg^{II} with dpa is available, but one notes the larger drop in log K_1 from the adpa to cdpa complex, suggesting that the Hg^{II}(adpa) complex is stabilized by a strong π contact.

The formation constants of Hg^{II} with cdpa in 50% MeOH/H_2O were measured by monitoring the fluorescence intensity of a 5×10^{-6} M solution of both $Hg(ClO_4)_2$ and cdpa over the pH range 2–12. Variation of the peak intensity at five different wavelengths with pH is seen in Figure 11. The intensity is quite low in the pH range 2–4, it rises strongly to pH 6, and then drops down again to pH 8.0. One can understand this behavior from the species distribution diagram in Figure 12. The higher intensity fluorescence of the Hg^{II}(cdpa) system between pH 4 and 8 appears to correspond to the presence of the Hg^{II}(cdpa) complex. One would expect a higher fluorescence intensity for this species because structure **6** shows that both fluorophores are not π-contacted with the Hg^{II} ion, and there are no long Hg–N bonds in the structure that might lead to a PET effect that quenches the fluorescence. The species distribution diagram in Figure 12 shows how the species present in a 1:1 Hg^{II}(cdpa) solution at a typical pH of 7.0 might be quite different from an assumption that in such a 1:1 solution one has mainly the Hg^{II}(cdpa) monospecies present. A more complete analysis of species present in solutions used for studying the fluorescent sensing of metal ions can make such studies much more informative and valuable in developing theories of how the CHEF effect operate in such systems.

Patterns of Hapticity for π Contacts of Different Metal Ions. The presence of η^2 π contacts in the Ag^I(cdpa) complex, and a η^1 π contact in the Ag^I(adpa) complex,[3] raises the question of what patterns of hapticity might exist for π contacts formed by Ag^I and other types of metal ions. The interest is to obtain a broad picture of what types of metal ions prefer low hapticities such as η^1 or η^2, on the one hand, and what types

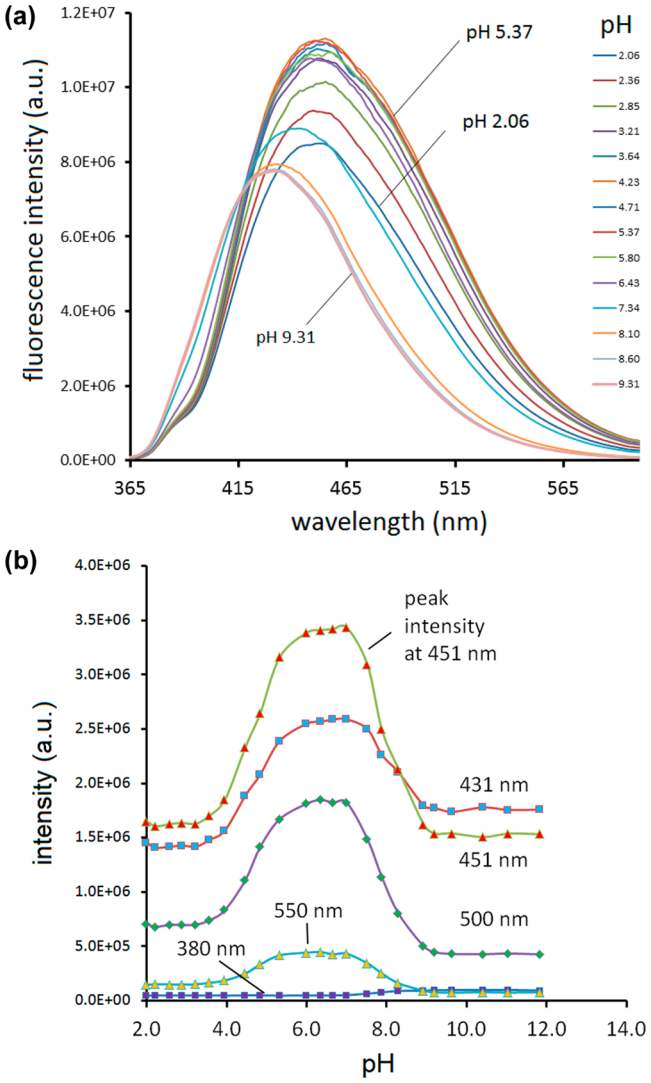

Figure 11. (a) Fluorescence spectra of 1:1 Hg^{II}/cdpa (5×10^{-6} M) in 50% MeOH/H_2O over the pH range 2.06–9.31. (b) Fluorescence intensity at five different wavelengths for 5×10^{-6} M $Hg(ClO_4)_2$ and cdpa in 50% MeOH/H_2O at 25 °C over the pH range 2.06–9.31. The pH region of increased fluorescence intensity appears to correspond with the pH region between pH 4 and 9, where the $[Hg(cdpa)_2]^{2+}$ and $[Hg(cdpa)(OH)]^+$ complexes are the dominant species, as suggested by Figure 12.

prefer high hapticities such as η^6, on the other hand. After examination of a large number of structures in the CSD,[11] a difference of more than 0.2 Å between the shortest contact present, and its adjacent contacts, was used to define a η^1 π contact. This choice is not critical because most contacts assigned as η^1 have much larger differences than the one with adjacent contacts: for example, the π contact of 3.018 Å in the Ag^I(adpa) complex, identified[3] as being a η^1 π contact, has Ag···C contacts on either side of it of 3.537 and 3.461 Å. One defines a η^2 π contact as having the shortest two adjacent contacts present, differing by no more than 0.2 Å from each other but being at least 0.2 Å shorter than any adjacent contacts present. Again, this does not appear to be a critical choice: in the Ag^I(cdpa) complex reported here, as a typical example, identified as having a η^2 π contact, the two Ag···C η^2 π contacts are 3.083 and 3.095 Å, while the two Ag···C contacts on either side of the two η^2 π contacts are 3.724 and 3.750 Å. Contacts of

DOI: 10.1021/acs.inorgchem.5b01766
Inorg. Chem. 2015, 54, 9976–9988

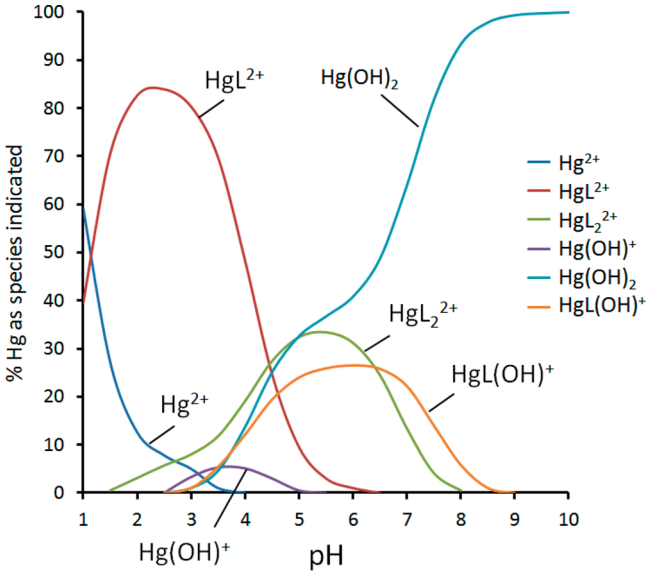

Figure 12. Species distribution diagram for the Hg^{II}(cdpa) (=L) system, both 5×10^{-6} M, calculated using the program *HySS*[30] and formation constants for Hg^{II} with cdpa determined here in 50% MeOH/H_2O, as seen in Table 8.

hapticity η^3–η^5 seemed uncommon with the metal ions examined here and so were not considered further. A η^6 set of π contacts was defined as having all six contacts within 0.5 Å of each other. Again, the latter choice does not appear to be crucial because, in most cases identified as η^6 π contacts, the differences are much smaller than that. The definition of hapticity adopted here allows for easy searching of the CSD and transfer of the results into the *Excel* program,[29] where automated assignment of the hapticity can be carried out.

The CSD was searched to determine the hapticty of a selection of metal ions when bound to benzene or simple aromatics such as xylenes or naphthalene. This was done to avoid more sterically constraining situations, where the observed hapticity may derive from the steric properties of a ligand with additional donor groups apart from the π-contacting aromatic. For example, Pb^{II} forms a η^1 π contact in its adpa complex,[3] even though with less sterically constraining aromatics such as xylenes it always forms η^6 π contacts, as seen in Table 10. In Table 10 are shown the hapticities observed in the CSD for a selection of metal ions with simple aromatics. It is apparent that d^{10} metal ions such as Cu^I, Ag^I, Au^I, Zn^{II}, Cd^{II}, and Hg^{II} form π contacts that, in the absence of additional constraining factors, are nearly always η^1 or η^2. More ionically bound metal ions, such as Na^I, K^I, Ba^{II}, La^{III}, or Th^{IV}, are nearly always η^6 π-contacted with simple aromatics. It appears that this arises from the more ionic bonding of the latter ions being electrostatically attracted to the general cloud of electron density present in the π system, whereas the more covalently bound d^{10} metal ions form more directed bonds to one or two C atoms, which may involve a σ-bonding component to the interaction.[48] One notes that square-planar or tetragonally distorted metal ions such as Cu^{II} and Pd^{II} in Table 10 appear to prefer η^1 π contacts, which may simply be due to the limited space available for the formation of π contacts on the axial coordination sites of these metal ions.

A further group of predominately η^6 π-contacted metal ions in the absence of sterically constraining factors appears from Table 10 to be the $d^{10}s^2$ metal ions such as Tl^I, Pb^{II}, and Bi^{III}.

Table 10. Hapticity[a] of Benzene Rings π-Contacted with a Selection of Metal Ions in Structures Located in the CSD[b],[1]

	no. of examples displaying the hapticity indicated					
metal ion	η^1	η^2	η^3	η^4	η^5	η^6
Na^I	1	0	0	0	0	**7**
K^I	1	0	0	0	0	**23**
Rb^I	1	0	0	0	0	**15**
Cu^I	**11**	**14**	0	0	0	0
Ag^I	**19**	**23**	0	0	0	0
Au^I	**10**	**9**	0	0	0	0
Tl^I	1	0	0	0	0	**19**
Ba^{II}	0	0	0	0	0	**48**
Zn^{II}	**9**	**3**	0	0	0	1
Cd^{II}	**3**	**2**	0	0	0	0
Hg^{II}	**54**	**46**	0	0	0	8
Pb^{II}	0	0	0	0	0	**10**
La^{III}	0	0	0	0	0	**6**
Bi^{III}	0	0	0	0	0	**10**
Th^{IV}	0	0	0	0	0	**4**
Cu^{II}	**25**	0	0	0	0	0
Pd^{II}	**4**	0	0	0	0	0

[a]The hapticity is defined as follows: η^1, shortest contact shorter than any other contact by at least 0.2 Å; η^2, two shortest contacts within 0.2 Å of each other and shorter than any other contacts by at least 0.2 Å; η^3, three shortest contacts within 0.2 Å of each other and shorter than any other contacts by at least 0.2 Å; η^6, all six contacts within 0.5 Å of each other. [b]Bold type indicates predominant hapticities of each metal ion.

For these metal ions, the structures suggest that the π-contacted aromatic rings coordinate near the site of the "inert pair" of electrons on the metal ion. One assigns the position of the inert pair by examining the structure for a "gap" in the coordination sphere and/or longer M–L bonds near the proposed site of the lone pair and shorter M–L bonds opposite the site.[31−33] The bonds near the lone pair on Pb^{II} are very long,[31−33] and it appears that these probably are also ionic and rather weakly directional and thus favor η^6 contacts.

Effects of the formation of π contacts on the structures of aromatic rings by the metal ions considered here appear to be minimal, as would be expected for fairly weak interactions.[48] An important parameter is the value of the C···C–H angle, involving the *p*-C atom across the aromatic ring from the *ipso*-C atom, where the π contact is formed, and the H atom attached to the *ipso*-C atom. Ideally, this angle should be 180°, but with formation of a π contact, the H atom may be bent away from the π-contacting metal ion, and the angle is decreased, decreasing more with increasing strength of the π contact.[48] With strong π contacts, such as η^1 Hg···C π contacts of as short as 2.269 Å, the C···C–H angle across the aromatic ring can be as little as 144.9° instead of the expected 180°, with the H atom on the *ipso*-C atom strongly bent away from the π-contacting Hg atom.[49,50] The Ag^I ion forms numerous fairly short Ag···C π contacts close to 2.49 Å, where the C···C–H angle across the aromatic ring is typically decreased by only about 2–3° compared to the expected value for the angle of 180°. In the mercury(II) dichloride complex of adpa, with a Hg···C π contact of 3.215 Å, the C···C–H angle is 175.7°, with the *ipso*-H atom bent away from the π-contacting Hg atom.[1] In the Ag^I complexes of adpa and cdpa, the decreases in the C···C–H angles are small, at 1.8° for the adpa complex[3] and 0.6° for the

DOI: 10.1021/acs.inorgchem.5b01766
Inorg. Chem. 2015, 54, 9976−9988

cdpa complex, consistent with the idea that the π contacts are rather weak.

CONCLUSIONS

(1) The order of π-contacting ability of the metal ions considered here appears to be $Zn^{II} \ll Cd^{II} < Pb^{II} < Hg^{II} < Pd^{II} \approx Cu^{II} \approx Ag^{I}$. The coumarin fluorophore cdpa is suggested by electrostatic potential maps to be a weaker M···C π contacter than the anthracenyl fluorophore of adpa: the order of ability to produce a CHEF effect with cdpa is $Zn^{II} \approx Cd^{II} > Pb^{II} > Hg^{II} \gg Ag^{I}$ (no CHEF effect) $\approx Cu^{II} \approx Ni^{II}$ compared to the order for adpa of $Zn^{II} > Cd^{II} \gg Pb^{II}$ (no CHEF effect) $\approx Hg^{II} \approx Ag^{I} \approx Cu^{II} \approx Ni^{II}$. With both cdpa and adpa, the paramagnetic Cu^{II} and Ni^{II} ions strongly quench the fluorescence, in line with a redox mechanism of quenching that does not appear to require the formation of M···C π contacts. (2) Crystallographically, only the Ag^{I}(cdpa) complex (**1**) shows M···C π contacts, in agreement with the observation that Ag^{I} strongly quenches the fluorescence of cdpa, while the other diamagnetic metal ions show CHEF effects. Importantly, Pb^{II} (**2**) shows in the solid-state structure of its cdpa mono-complex no M···C π contacts with the fluorophore of cdpa, and also shows a CHEF effect. In contrast, the Pb^{II}(adpa) complex shows an M···C π contact and so shows no CHEF effect.[3] (3) The observation of cdpa bis-complexes in **5** and **6** in spite of crystal growth from solutions that had 1:1 molar ratios of metal ion and cdpa raises the question of what species might be present in such solutions. It is clear that, if one wishes to understand the CHEF effect in fluorescent sensors for metal ions, it is important to establish that the complex in solution is completely formed and also to understand the speciation of the solution. One might otherwise, for example, conclude that a metal ion such as Hg^{II} showed no CHEF effect with the sensor, when, in fact, it had not formed a complex.

ASSOCIATED CONTENT

Supporting Information

The Supporting Information is available free of charge on the ACS Publications website at DOI: 10.1021/acs.inorgchem.5b01766.

X-ray crystallographic data in CIF format (CIF)
X-ray crystallographic data in CIF format (CIF)
X-ray crystallographic data in CIF format (CIF)
X-ray crystallographic data in CIF format (CIF)
X-ray crystallographic data in CIF format (CIF)

AUTHOR INFORMATION

Corresponding Author

*E-mail: hancockr@uncw.edu.

Notes

The authors declare no competing financial interest.

ACKNOWLEDGMENTS

The authors thank the University of North Carolina—Wilmington for support for this research and a bursary to J.W.N. Dr. Robert Whitehead is thanked for his assistance with elemental analyses of the complexes synthesized. Dr. Jiangnan Peng is thanked for assistance with mass spectrometry, and the NSF Division of Chemistry is thanked for providing the mass spectrometer used under Grant CHE1039784.

REFERENCES

(1) Lee, H.; Lee, H.-S.; Reibenspies, J. H.; Hancock, R. D. *Inorg. Chem.* **2012**, *51*, 10904.
(2) Nugent, J. W.; Lee, H.; Lee, H.-S.; Reibenspies, J. H.; Hancock, R. D. *Chem. Commun.* **2013**, *49*, 9749.
(3) Nugent, J. W.; Lee, H.; Lee, H.-S.; Reibenspies, J. H.; Hancock, R. D. *Inorg. Chem.* **2014**, *53*, 9014.
(4) Lee, H.; Hancock, R. D.; Lee, H.-S. *J. Phys. Chem. A* **2013**, *117*, 13345.
(5) Hancock, R. D. *Chem. Soc. Rev.* **2013**, *42*, 1500.
(6) de Silva, A. P.; Gunaratne, H. Q. N.; Gunnlaugsson, T.; Huxley, A. J. M.; McCoy, C. P.; Rademacher, J. T.; Rice, T. E. *Chem. Rev.* **1997**, *97*, 1515.
(7) Takashima, I.; Kinoshita, M.; Kawagoe, R.; Nakagawa, S.; Sugimoto, M.; Hamachi, I.; Ojida, A. *Chem. - Eur. J.* **2014**, *20*, 2184.
(8) Hitomi, Y.; Nagai, T.; Kodera, M. *Chem. Commun.* **2012**, *48*, 10392.
(9) Elliott, E. K.; Hu, J.; Gokel, G. W. *Supramol. Chem.* **2007**, *19*, 175.
(10) (a) Lim, N. C.; Bruckner, C. *Chem. Commun.* **2004**, 1094. (b) Lim, N. C.; Schuster, J. V.; Porto, M. C.; Tanudra, M. A.; Yao, L.; Freake, H. C.; Bruckner, C. *Inorg. Chem.* **2005**, *44*, 2018.
(11) *Cambridge Structural Database*; Cambridge Structural Database: Cambridge, United Kingdom, 2013.
(12) Hancock, R. D.; Reibenspies, J. H.; Maumela, H. *Inorg. Chem.* **2004**, *43*, 2981.
(13) Luckay, R.; Cukrowski, I.; Mashishi, J.; Reibenspies, J. H.; Bond, A. H.; Rogers, R. D.; Hancock, R. D. *J. Chem. Soc., Dalton Trans.* **1997**, 90.
(14) Greenwood, N. N.; Earnshaw, A. *Chemistry of the Elements*, 2nd ed.; Butterworth: Oxford, U.K., 2001; p 1218.
(15) Wiosna, G.; Petkova, I.; Mudadu, M. S.; Thummel, R. P.; Waluk, J. *Chem. Phys. Lett.* **2004**, *400*, 379.
(16) Waluk, J. *Acc. Chem. Res.* **2003**, *36*, 832.
(17) Hedges, J. I.; Stern, J. H. *Limnol. Oceanogr.* **1984**, *29*, 657.
(18) Gabe, E. J.; Le Page, Y.; Charland, J.-P.; Lee, F. L.; White, P. S. *J. Appl. Crystallogr.* **1989**, *22*, 384.
(19) *FluorEssence program*, version 2.1; Horiba Jobin Yvon, Inc.: Edison, NJ, 2006.
(20) *ORTEP-3 for windows - a version of ORTEP-III with a graphical user interface (GUI)*: Farrugia, L. J. *J. Appl. Crystallogr.* **1997**, *30*, 565.
(21) *Spartan 14* from Wavefunction, Inc., Irvine, CA: Shao, Y. *Phys. Chem. Chem. Phys.* **2006**, *8*, 3172.
(22) Lee, C.; Yang, W.; Parr, R. G. *Phys. Rev. B: Condens. Matter Mater. Phys.* **1988**, *37*, 785.
(23) Becke, A. D. *J. Chem. Phys.* **1993**, *98*, 5648.
(24) Hehre, W. J.; Ditchfield, R.; Pople, J. A. *J. Chem. Phys.* **1972**, *56*, 2257.
(25) Hay, P. J.; Wadt, W. R. *J. Chem. Phys.* **1985**, *82*, 270.
(26) Wadt, W. R.; Hay, P. J. *J. Chem. Phys.* **1985**, *82*, 284.
(27) Hay, P. J.; Wadt, W. R. *J. Chem. Phys.* **1985**, *82*, 299.
(28) *HyperChem program*, version 8.0; Hypercube Inc.: Waterloo, Ontario, Canada.
(29) Billo, E. J. *Excel for Chemists*; Wiley-VCH: New York, 2001.
(30) Alderighi, L.; Gans, P.; Ienco, A.; Peters, D.; Sabatini, A.; Vacca, A. *Coord. Chem. Rev.* **1999**, *184*, 311.
(31) Shimoni-Livny, L.; Glusker, J. P.; Bock, C. W. *Inorg. Chem.* **1998**, *37*, 1853.
(32) Hancock, R. D.; Reibenspies, J. H.; Maumela, H. *Inorg. Chem.* **2004**, *43*, 2981.
(33) Hancock, R. D.; Salim Shaikjee, M.; Dobson, S. M.; Boeyens, J. C. A. *Inorg. Chim. Acta* **1988**, *154*, 229.
(34) Tewari, A. K.; Srivastava, P.; Singh, V. P.; Singh, P.; Khanna, R. S. *Res. Chem. Intermed.* **2013**, *39*, 2925.
(35) Dubey, R.; Lim, D. *Curr. Org. Chem.* **2011**, *15*, 2072.
(36) Janiak, C. *Dalton* **2000**, *21*, 3885.
(37) Asensio, J. L.; Arda, A.; Canada, F. J.; Jimenez-Barbero, J. *Acc. Chem. Res.* **2013**, *46*, 946.
(38) Eom, G. H.; Kim, J. H.; Jo, Y. D.; Kim, E. Y.; Bae, J. M.; Kim, C.; Kim, S.-J.; Kim, Y. *Inorg. Chim. Acta* **2012**, *387*, 106.

DOI: 10.1021/acs.inorgchem.5b01766
Inorg. Chem. 2015, 54, 9976−9988

(39) Cockrell, G. M.; Zhang, G.; VanDerveer, D. G.; Thummel, R. P.; Hancock, R. D. *J. Am. Chem. Soc.* **2008**, *130*, 1420.
(40) Carolan, A. N.; Cockrell, G. M.; Williams, N. J.; El Ojaimi, M.; VanDerveer, D. G.; Thummel, R. P.; Hancock, R. D. *Inorg. Chem.* **2013**, *52*, 15.
(41) Martell, A. E.; Smith, R. M. *Critical Stability Constant Database, 46*; National Institute of Science and Technology (NIST): Gaithersburg, MD, 2003.
(42) Anderegg, G.; Hubmann, E.; Podder, N. G.; Wenk, F. *Helv. Chim. Acta* **1977**, *60*, 123.
(43) Shannon, R. D. *Acta Crystallogr., Sect. A: Cryst. Phys., Diffr., Theor. Gen. Crystallogr.* **1976**, *32*, 751.
(44) Bebout, D. C.; De Lanoy, A. E.; Ehmann, D. E.; Kastner, M. E.; Parrish, D. A.; Butcher, R. J. *Inorg. Chem.* **1998**, *37*, 2952.
(45) Glerup, J.; Goodson, P. A.; Hodgson, D. J.; Michelsen, K.; Nielsen, K. M.; Weihe, H. *Inorg. Chem.* **1992**, *31*, 4611.
(46) Wilhelm, M.; Deeken, S.; Berssen, E.; Saak, W.; Lutzen, A.; Koch, R.; Strasdeit, H. *Eur. J. Inorg. Chem.* **2004**, *2004*, 2301.
(47) Helm, M. L.; Loveday, K. D.; Combs, C. M.; Bentzen, E. L.; Van Derveer, D. G.; Rogers, R. D.; Grant, G. J. *J. Chem. Crystallogr.* **2003**, *33*, 447.
(48) Hubig, S. M.; Lindeman, S. V.; Kochi, J. K. *Coord. Chem. Rev.* **2000**, *200*−*202*, 831.
(49) Borovik, A. S.; Bott, S. G.; Barron, A. R. *J. Am. Chem. Soc.* **2001**, *123*, 11219.
(50) Borovik, A. S.; Bott, S. G.; Barron, A. R. *Angew. Chem., Int. Ed.* **2000**, *39*, 4117.

DOI: 10.1021/acs.inorgchem.5b01766
Inorg. Chem. 2015, 54, 9976−9988